We are IntechOpen, the world's leading publisher of Open Access books Built by scientists, for scientists

4,800
Open access books available

122,000
International authors and editors

135M
Downloads

Our authors are among the

154
Countries delivered to

TOP 1%
most cited scientists

12.2%
Contributors from top 500 universities

CLARIVATE ANALYTICS BOOK CITATION INDEX INDEXED

WEB OF SCIENCE™

Selection of our books indexed in the Book Citation Index in Web of Science™ Core Collection (BKCI)

Interested in publishing with us?
Contact book.department@intechopen.com

Numbers displayed above are based on latest data collected.
For more information visit www.intechopen.com

2

Neuroimaging in Inborn Errors of Metabolism

Carlos Casimiro, Paula Garcia, Miguel Cordeiro,
Isabel Fineza, Teresa Garcia and Luísa Diogo
Centro Hospitalar Universitário de Coimbra
Portugal

1. Introduction

Inborn errors of metabolism (IEM) are a heterogeneous group of genetic disorders, classically caused by enzyme deficiency. They are associated with different pathogenic mechanisms from enzyme substract accumulation or product deficiency to formation of an abnormal, toxic molecule. Occasionally, the deficient protein has non-enzymatic functions such as membrane transport or others, making the boundaries of IEM difficult to establish. IEM are individually rare (orphan diseases) but relatively numerous as a group, since more than 500 different entities have been identified (Scriver et al., 2001). Overall, their incidence is estimated to be 1:1,500 (Raghuveer et al., 2006).

The age of onset varies. Signs and symptoms of IEM present a considerable overlap among the diverse IEM and many other diseases, not allowing the differential diagnosis on a clinical basis. There is no correlation between genotype and phenotype, in general. Most symptoms are apparent at or soon after birth, but clinical onset may occur prenatally or at any age, including adulthood. Multisystem involvement is frequent, with the presence of nervous system manifestations in most patients, either at disease onset or during the evolution.

IEM are most probably underdiagnosed. In spite of all contributions from varied fields of medical science, etiological diagnosis is not achieved in a significant percentage of suspected patients. Despite being frequently difficult, diagnosis may be done selectively based on clinical features or pre-symptomatically by neonatal screening and achieved by biochemical, enzymatic and/or genetic studies. The diagnosis of IEM is challenging due to their rarity and clinical heterogeneity. To address these diagnostic problems, several schemes based on clinical, biochemical, neuroradiological, morphologic, enzymatic and genetic criteria have been proposed.

Neuroimaging techniques are essential for assessing brain structures, namely white matter and/or gray matter involvement (Barkovich, 2007). They are undoubtedly useful in neurologically affected patients' diagnosis and follow-up. Neuroradiological features of many IEM overlap and are stage-dependent. Patients occasionally show distinctive patterns of central nervous system involvement in magnetic resonance imaging (MRI). These patterns may characterise some disorders, especially during the early stages, or they can show guiding characteristics, or reveal non-specific changes. In later phases, the MRI findings are similar for most IEM with neurological involvement, often presenting diffuse loss of brain tissue and increased water in the remaining tissue. For this reason, it is

important to submit the patient to a brain MRI early in the course of the disease, when some key features are more evident (Barkovich, 2007).
Although the majority of patients present non-specific changes on MRI, a systematic pattern recognition approach to involved brain structures is useful, as it narrows differential diagnosis. It occasionally points to a diagnosis and allows the reduction of the biochemical and genetic work-ups. According to brain MRI in early stages, IEM can be classified into disorders primarily involving gray matter, diseases primarily involving white matter and disorders involving both gray matter and white matter (Barkovich, 2006, 2007). The proton magnetic resonance spectroscopy (MRS) may be more sensitive to detect early abnormalities in the brain. However, only a few metabolic diseases present with specific MRS findings.
Other neuroimaging techniques, such as positron emission tomography (PET) and single photon emission computed tomography (SPECT), could be useful in the diagnosis and follow-up of IEM. Nonetheless, they are not widely available on a routine clinical basis.
This section will review the most relevant IEM, based on a practical pattern-recognition approach to brain MRI and its correlation to clinical, biochemical and genetic features.

2. Disorders primarily involving gray matter

IEM primarily involving gray matter, known as poliodystrophies, can affect cortical or deep gray matter in the early phases. This differentiation should be made in order to accurately discriminate a range of diseases.

2.1 Disorders primarily involving cortical gray matter

During an acute phase, neuroimaging reveals sulcal effacement, cortical swelling and restricted diffusion when the damage affects primarily the cortical gray matter (Barkovich, 2005). The imaging findings during a chronic phase are: sulcal volume increasing, cortical thinning and cortical low attenuation on computed tomography (CT) scan, and T1 and T2 prolongation on MRI (Campistol, 1999). Nevertheless, in later phases, lesions can progress and spread to other brain structures (including deep gray matter, white matter and the cerebellum) (van der Knaap & Valk, 2005), showing non-specific patterns.
The primary involvement of cortical gray matter is commonly found in neuronal ceroid lipofuscinoses, mucolipidosis type I and GM1 gangliosidosis. Generally, findings on imaging studies are non-specific in these disorders.

2.1.1 Neuronal ceroid lipofuscinoses

The neuronal ceroid lipofuscinoses (NCL) are inherited lysosomal storage diseases characterized by the accumulation of autofluorescent ceroid lipopigments in the lysosomes of neurons and other cell types. Together, they constitute the commonest group of progressive neurodegenerative diseases in children, and are inherited in an autosomal recessive mode. The adult form of NCL is rare and demonstrates either an autosomal recessive or a dominant mode of inheritance (Haltia, 2003). The main features of these diseases include visual failure, seizures, progressive physical and mental decline, and premature death. Diagnosis, based on the age of clinical presentation, is made by enzymatic or genetic studies. Ultra-structural analysis of white blood cells or skin can be used to orientate biochemical and genetic tests in atypical cases (Williams et al., 2006).

The major imagiological features in NCL are cerebral and cerebellar atrophy, cortical thinning associated with mild hyperintensity of the cerebral white matter and hipointensity of the thalami on T2-weighted images (T2-WI) (Incerti, 2000). Infantile and late infantile variants show rapid progression of enlargement of ventricles and sulci of the brain. In the juvenile and adult forms, however, cerebral atrophy is frequently slight in the course of the disease, or may remain totally absent (Autti et al., 1996). Cerebellar atrophy is common and may be the earliest finding in late-infantile and juvenile forms of NCL. In late infantile form, the first finding is usually a rapid progression of cerebellar atrophy (Fig. 1.), whilst in infantile and juvenile forms this progression is slower (Järvelä et al., 1997). T2-WI hyperintensity in white matter, which is usually less intense than in leukodystrophies, tends to spare the subcortical areas and initially involves the posterior periventricular region. Later in the disease, corpus callosum may also become thinner (Incerti, 2000).

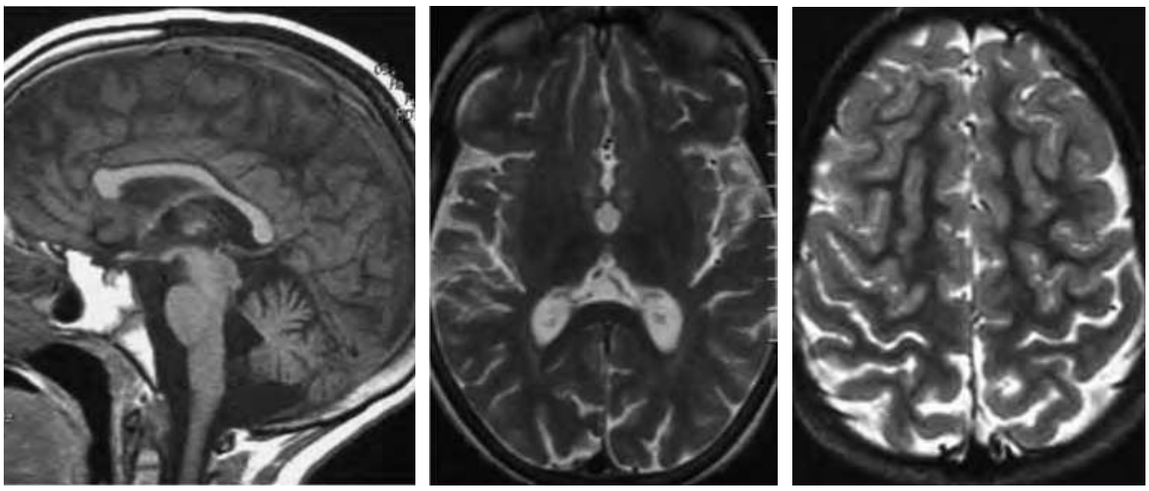

(a) (b) (c)

Fig. 1. Late infantile NCL. (a) Midline sagittal T1-WI demonstrates cerebellar atrophy. Axial T2-WI show mild thalamic hypointensity (b) and cortical thinning (c).

Diffusion-weighted imaging (DWI) can be very useful in detecting variances in abnormalities of cerebral water diffusion in the late infantile form, showing increased whole-brain apparent diffusion coefficient (ADC) values. It correlates with patient's age, disease severity and duration (Dyke et al., 2007). MRS can give additional hints to the diagnosis of infantile and late infantile forms, and be helpful in the differential diagnosis. In infantile NCL, MRS spectrum revealed progressive changes, with a complete loss of N-acetylaspartate (NAA), as well as marked reduction of creatine and choline, and increase in myo-inositol and lactate in gray matter and white matter. In late-infantile NCL, MRS spectrum revealed reduction of NAA in gray matter and white matter and an increase of myo-inositol, creatine and choline in white matter (Brockmann et al., 1996).

2.2 Disorders primarily involving deep gray matter

When the damage primarily affects the deep gray matter, neuroimaging reveals many different patterns, with involvement of particular structures. Some of them are more specific in a group of diseases, allowing for the narrowing in differential diagnosis. CT scan can be

normal, or disclose calcifications or hypodensity areas in deep gray matter. MRI sensibility is higher, although CT is best suited for calcification detection.
The list of IEM affecting deep gray matter is extensive. Globus pallidus hyperintensity in T2-WI can be seen in succinic semialdehyde dehydrogenase deficiency, methylmalonic acidemia, urea cycle disorders, guanidinoacetate methyltransferase deficiency, pyruvate dehydrogenase deficiency and isovaleric acidemia (Barkovich, 2005, 2007). Additionally, globus pallidus hypointensity, with or without central hyperintensity, is highly characteristic of Hallervorden-Spatz disease. Striatum hyperintensity in T2-WI can be seen in some mitochondrial respiratory chain disorders (MRCD) such as Leigh's syndrome and mitochondrial encephalopathy with lactic acidosis and stroke-like episodes – MELAS, the glutaric acidurias, propionic acidemia and molybdenum co-factor deficiency (Barkovich, 2005, 2007). Many of these IEM can concomitantly involve the white matter so some will be discussed later in this chapter.

2.2.1 Pantothenate kinase-associated neurodegeneration

Pantothenate kinase-associated neurodegeneration (PKAN), formerly known as Hallervorden-Spatz disease is an autosomal recessive disorder characterized by neurodegeneration with brain iron accumulation. Many patients have mutations in the pantothenate kinase 2 gene (PANK2). Two distinct groups were identified. Classical PKAN presents in early childhood, usually before age 6 years, has uniform presentation and is characterized by rapid progression of extrapyramidal and pyramidal signs, intellectual impairment, pigmentary retinal degeneration and abnormal eye movements. Atypical PKAN, which is less common, has a wider clinical spectrum and slower progression. PANK2 mutations are associated with all classic PKAN and one third of atypical disease cases (Hayflick et al., 2003). PKAN is suggested by typical MRI features, and the diagnosis is made by molecular genetic testing (Zhang et al., 2006).

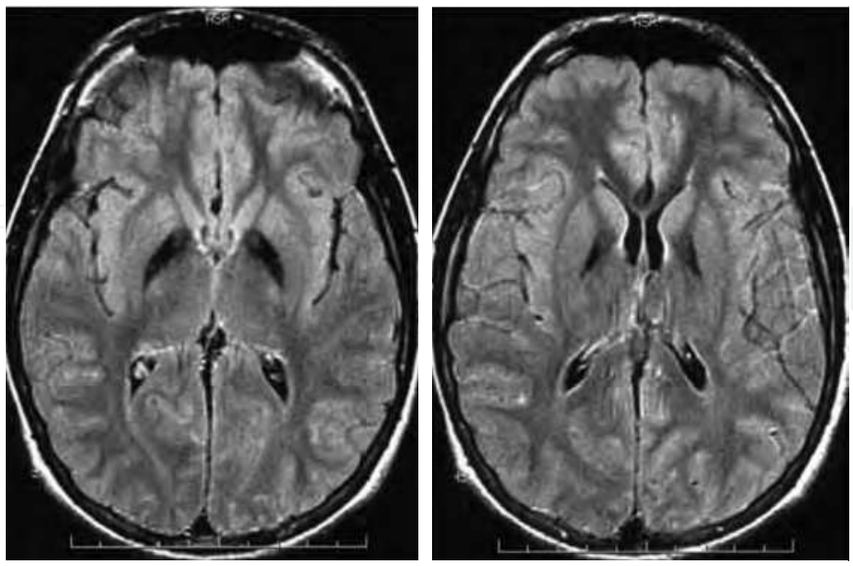

(a) (b)

Fig. 2. Pantothenate kinase-associated neurodegeneration (PKAN). (a) and (b) Axial FLAIR show hypointensity with a central region of hyperintensity in the globus pallidi.

Some patients' CT scans show low or high density areas in the globus pallidus. Low-density foci are a sign of tissue destruction, while the high-density foci reflect dystrophic calcification (Barkovich, 2005). All patients with PANK2 mutations had the specific pattern of T2-WI globus pallidus central hyperintensity (destruction and gliose) with surrounding hypointensity (iron deposition), known as the *eye-of-the-tiger* sign (Fig. 2.). This sign was not present in patients without mutations. Patients with PANK2 mutations could be distinguished by the occurrence of isolated globus pallidus hyperintensity on T2-WI before the hypointensity developed (Hayflick et al., 2006). Patients without PANK2 mutations revealed globus pallidus T2-WI hypointensity, without central hyperintensity. In the later stage of the disease, it can be seen evidence of iron deposition in the substantia nigra pars reticulata, cerebral and cerebellar atrophy. These signs were frequently and more severely seen in PANK2 mutation-negative patients (Hayflick et al., 2006).

MRS can show markedly decreased NAA/creatine ratio in the globus pallidus and substancia nigra, with increased myo-inositol/creatine ratio (Parashari et al., 2010).

2.2.2 Creatine deficiency syndromes

Creatine deficiency syndromes (CDS) are a newly described group of IEM affecting creatine metabolism. Three disorders have been described: guanidinoacetato methyltransferase (GAMT) deficiency, arginine:glycine amidinotransferase (AGAT) deficiency and creatine transporter defect (SLC6A8). GAMT e AGAT deficiencies (creatine synthesis pathway) have an autosomal recessive inheritance, whereas SLC6A8 defect is an X-linked disorder. All CDS can cause developmental delay, intellectual disability, behavioural problems, movement disorders, seizures, and severe disturbance of expressive language (Schulze, 2003). These clinical manifestations can be partially reversed by oral creatine supplementation and dietary manipulation, even in same patients with the creatine transporter defect (Chilosi et al., 2008; Mercimek-Mahmutoglu et al., 2010). CDS are suggested by marked reduction or complete absent of the creatine peak on MRS. Diagnosis relies on measurement of guanidinoacetate, creatine, and creatinine in urine and plasma and molecular genetic testing of the gene involved. If molecular test results are inconclusive, AGAT enzyme activity, GAMT enzyme activity, or creatine uptake in fibroblasts can be evaluated (Mercimek-Mahmutoglu & Stöckler-Ipsiroglu, 2009).

MRI and mainly MRS are very important tools to suggest CDS diagnosis and follow therapy response (Chilosi et al., 2008). In GAMT deficiency MRI can be normal or reveal T2-WI hyperintensity on globus pallidus, mild myelination delay or white matter hyperintensity. MRI is normal in AGAT deficiency (Barkovich, 2005); SLC6A8 defect MRI can show brain atrophy (Póo-Argüelles et al., 2006).

MRS shows spectrum changes even without MRI signal abnormally. Markedly reduction or absence of creatine peak, which is easily seen on long echo time (TE) spectrum, is the classical sign shared by all three disorders, in gray matter and white matter. GAMT deficiency reveals a broad guanidinoacetate peak at 3.78 ppm, on short TE sequences, which can be reduced (but not normalized) with dietary restriction of arginine associated to the supplementation of creatine and ornithine. In GAMT and AGAT deficient patients, but not in most of those with SLC6A8 deficiency, the creatine peak slowly increases under treatment (Fig. 3.).

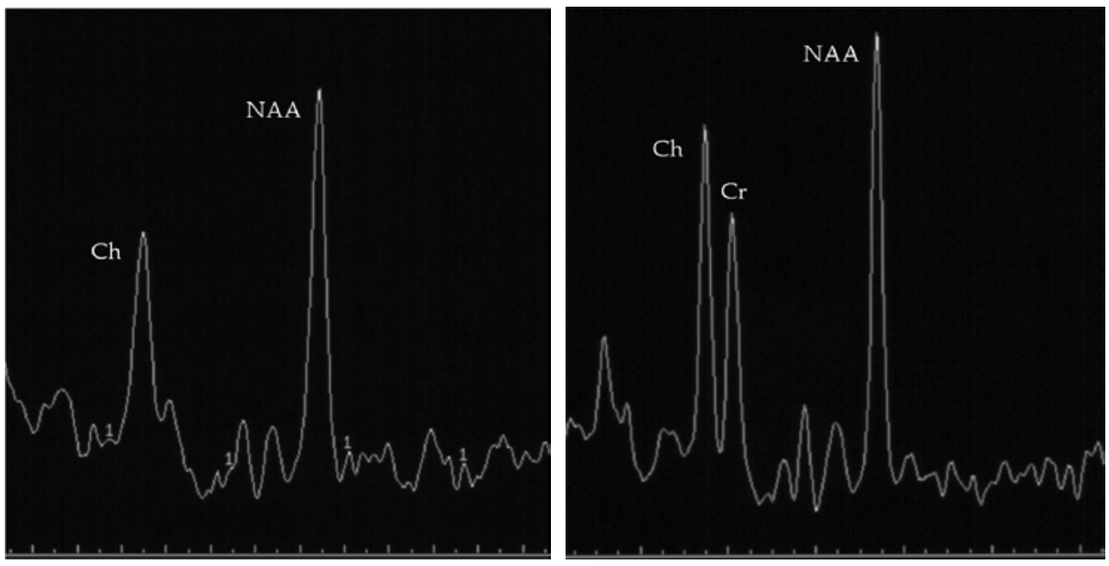

(a) (b)

Fig. 3. Creatine deficiency due to GAMT deficiency. (a) Multivoxel MRS spectrum (TE =144 ms) of the basal ganglia, before therapy, shows a markedly reduced creatine peak, and normal choline (Ch) and NAA peaks. (b) Multivoxel MRS spectrum (TE = 144 ms) of the basal ganglia, after 6 months therapy, shows a creatine (Cr) peak increasing.

3. Disorders primarily involving white matter

When the damage affects primarily the white matter, there is hypodensity on CT scan, and T1 and T2 prolongation on MRI. In later phases, the atrophy is the main feature. Knowledge of normal brain myelination, its appearance on different MRI sequences and normal variations, is crucial to accurately approach the range of disorders primarily involving white matter. When the damage affects primarily the white matter, it is important to find out if the white matter has never myelinated completely (hypomyelination), or if the myelin has been developed and destroyed afterwards (demyelination) (Barkovich, 2007). Since many of these IEM can also involve the gray matter, some will be discussed later in this chapter.

3.1 Hypomyelination diseases

The hypomyelination is observed in a small number of IEM, like Pelizaeus-Merzbacher disease and Salla disease. MRS findings may be useful in their differentiation (Barkovich, 2005).

3.1.1 Pelizaeus-Merzbacher disease

Pelizaeus-Merzbacher disease (PMD) is a recessive X-linked neurological disorder caused by a mutation in the proteolipidic protein 1 (PLP1) gene, which results in defective central nervous system myelination. The connatal PMD phenotype presents during the neonatal period or in the first weeks of life, with nystagmus, stridor, hypotonia, severe spasticity and motor deficits, cognitive impairment, seizures and, later on, absence of speech. Death usually occurs in the period from infancy to third decade. The classic PMD phenotype presents in the first 5 years of life, with nystagmus, hypotonia, titubation, ataxia, slow motor

development and extrapyramidal movements, like dystonia and athetosis. Death usually occurs between the third and the seventh decades. PMD is suggested by typical neurologic findings, X-linked inheritance pattern, and general changes on MRI. Molecular genetic testing of PLP1 is also available.

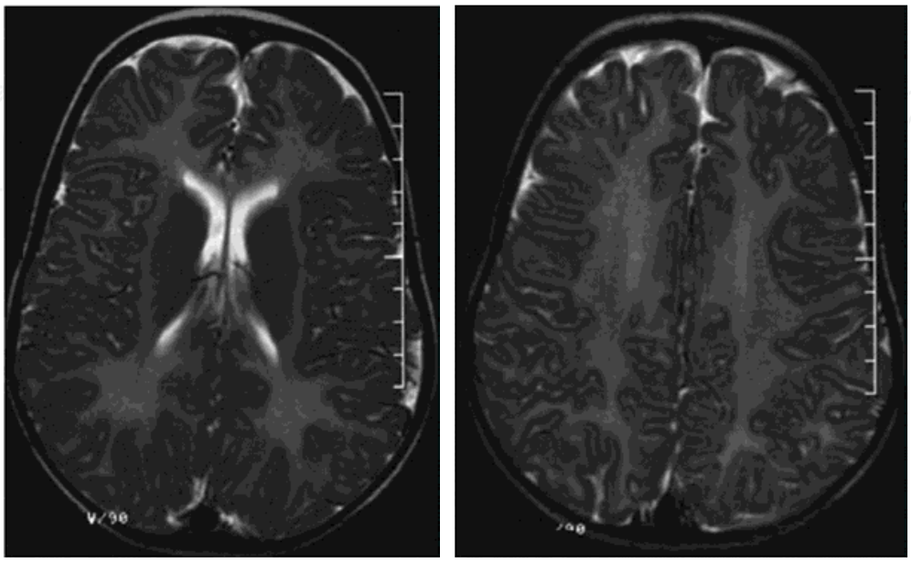

(a) (b)

Fig. 4. Pelizaeus-Merzbacher disease. (a) and (b) Axial T2-WI show abnormal high signal intensity in cerebral white matter, representing hypomyelination.

As in most white matter diseases, CT scan changes are non-specific, revealing white matter hypodensity and atrophy in later stages. MRI shows discordance of myelin maturation caused by a lack of myelination. In the connatal form, a complete absence of myelin in the brain is demonstrated (Fig. 4.) (van der Knaap & Valk, 1989). In classical forms in the early stages, MRI shows a brain with normal appearance, but more immature than expected. During infancy, myelin development of the brain progresses in an orderly and predictable fashion. Absence of these predictable patterns should raise the consideration for PMD. In late and severe cases, MRI reveals diffusely T2 hyperintensity and generalized volume reduction in the white matter with thinned corpus callosum and cortical sulci enlargement (Plecko et al., 2003).

MRS is very useful for evaluating both axonal integrity and myelination. However, reports may vary, which might be related to different clinical phenotypes, genotypes, or stages of disease progression (Pizzini et al, 2003). The pattern of metabolite abnormalities in individuals with PLP1 duplication appears to be distinctive, showing increased levels of NAA, creatine, glutamine and myo-inositol, which helps the differentiation of PMD from other leukodystrophies (Hanefeld et al., 2005).

3.2 Demyelination diseases

MR imaging has become the primary imaging modality in demyelinating diseases, playing an essential role in the identification, localization, and characterization of these pathologies. Demyelination processes can primarily involve subcortical white matter or periventricular

white matter. This differentiation should be made to ensure an effective imagiological approach and facilitate differential diagnosis.

3.2.1 Disorders primarily involving subcortical cerebral white matter

Early subcortical white matter demyelination can be seen in megalencephalic leukoencephalopathy with subcortical cysts, Alexander disease, some organic acidurias, Kearns-Sayre syndrome, galactosemia and diverse MRCD.

3.2.1.1 Megalencephalic leukoencephalopathy with subcortical cysts

Megalencephalic leukoencephalopathy with subcortical cysts (MLC), also known as van der Knaap disease, is an autosomal recessive disorder caused by mutations in the MLC1 gene. This gene encodes a protein mainly expressed in astrocytic endfeet at the blood-brain and cerebrospinal fluid-brain barriers (Boor et al., 2007). MLC is characterized by development of macrocephaly through the first year of life, generally up to the 98th percentile. Head circumference stabilizes afterwards. Initially, the psychomotor development is relatively normal or only mildly delayed. Later on, motor development delay, cerebellar ataxia, dysarthria, spasticity, and sometimes extrapyramidal signs ensue. Seizures, usually responsive to medication, are also observed in some children. MLC diagnosis can be made by recognition of typical neurologic signs and symptoms, and its distinguished brain MRI features. Molecular genetic testing of MLC1 is available (van der Knaap & Scheper, 2008).

The MRI is characterized by diffusely abnormal and mildly swollen cerebral white matter, showing enlargement of the gyri, and subcortical cysts in posterior frontal and temporal lobes (Barkovich, 2005). Central white matter is better preserved, especially the corpus callosum, internal capsule and brainstem. The presence of cerebellar white matter T2 hyperintensity is mild. Follow-up MRI reveals cerebral atrophy, and subcortical cyst growth can be present in some cases (van der Knaap et al, 1995).

Abnormal white matter shows increased diffusivity on DWI (Gelal, 2002). MRS reveals reduced NAA in T2 hyperintensity areas (Morita et al., 2006).

Tc-99m-ethyl cysteinate dimer SPECT reveals hypoperfusion in the abnormal cerebral white matter seen on MRI (Kiriyama et al., 2007).

3.2.1.2 Alexander disease

Alexander disease, or fibrinoid leukodystrophy, is caused by a gene mutation encoding glial fibrillary acidic protein (GFAP), leading to profound cellular dysfunction (Cecil & Kos, 2006). The pathological hallmark is the accumulation of ubiquitinated intracytoplasmic inclusions in astrocytes, called Rosenthal fibers. The infantile form, the most frequent, is present in the first 2 years of life, typically with macrocephaly and frontal bossing, psychomotor retardation, seizures, pyramidal signs and ataxia. Patients survive weeks to several years. Diagnosis is based on MRI features. Molecular genetic testing, for GFAP gene, is available (Gorospe, 2010).

CT scan shows low attenuation in frontal white matter with posterior progression to involve parietal region, internal capsules, and sometimes caudate heads. Frequently the tips of frontal horns show contrast-enhancement. There are 5 criteria on MRI to diagnose Alexander disease, according to van der Knaap: (1) extensive cerebral white matter changes with frontal predominance; (2) a periventricular rim with high signal on T1-WI and low signal on T2-WI; (3) signal abnormalities with swelling or volume loss in the basal ganglia and thalami; (4) brainstem signal abnormalities; and (5) contrast enhancement of one or

more of the following structures: ventricular lining, periventricular rim tissue, white matter of the frontal lobes, optic chiasm, fornix, basal ganglia, thalamus, dentate nucleus, or brainstem structures. The association of 4 or more criteria is relatively specific for Alexander disease. The imagiological pattern of enhancement provides specific information that can lead to correct diagnosis. Subcortical white matter is affected early in the course of the disease. The frontal changes correspond to prolonged T1 and T2 relaxation times, and tend to involve the parietal white matter and the internal and external capsules (van der Knaap et al., 2001). The progression of disease can lead to cavitations in the white matter (Vargas, 2009).
DWI reveals increased diffusion in the affected regions (Barkovich, 2005). MRS shows elevated myo-inositol and decreased NAA in the lesions (Cecil & Kos, 2006).

3.2.2 Disorders primarily involving periventricular cerebral white matter

Early periventricular white matter lesions can be seen in Krabbe disease, GM2 gangliosidoses, metachromatic leukodystrophy, X-linked adrenoleukodystrophy, vanishing white matter disease, phenylketonuria, maple syrup urine disease, Lowe syndrome, Sjögren-Larsson syndrome and mucolipidosis type IV.

3.2.2.1 Metachromatic leukodystrophy

Metachromatic leukodystrophy (MLD) is a lysosomal storage disease caused by decreased activity of arylsulfatase A, resulting in failure of myelin breakdown and reutilization in the central and peripheral nervous systems. There are three clinical forms: late infantile MLD (50-60% of the cases), juvenile MLD (20-30%), and adult MLD (15-20%) (Fluharty, 2008). The late infantile MLD presents before age 2 years with weakness, hypotonia, delayed psychomotor development, impairment of speech, spasticity, seizures and compromised vision and hearing. Death usually occurs before age 5. MLD is suspected by neurodegeneration and evidence

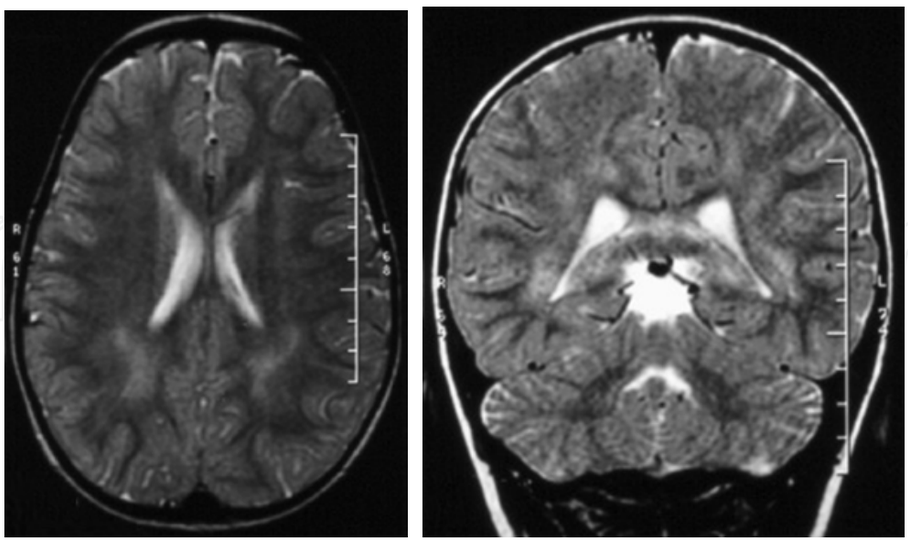

(a) (b)

Fig. 5. Metachromatic leukodystrophy. Axial (a) and coronal (b) T2-WI show abnormal hyperintensity in the periventricular white matter, predominantly around the posterior body and trigones of the lateral ventricles, sparing subcortical U fibers.

of leukodystrophy on MRI. Diagnosis is suggested by increased urinary excretion of sulfatides and/or decreased arylsulfatase A activity, and is confirmed by genetic testing. Metachromatic lipids deposits can be seen in the nervous system tissue (Fluharty, 2008).
CT scan shows confluent attenuation of periventricular white matter density. MRI reveals progressive symmetrical prolongation of T1 and T2 relaxation times in periventricular white matter. The cerebral white matter located around the posterior body and trigones of lateral ventricles is involved earlier in late infantile MLD (Fig. 5.), whereas frontal white matter is involved in cases of late onset. Subcortical U fibers are spared early but not in the later stages of the disease course. No enhancement has been reported. Later signs include cerebral atrophy. Higher resolution images reveal *leopard skin* pattern or *tigroid* pattern in the centrum semiovale that correspond to areas combining demyelination and normal regions. The progression of disease leads to involvement of the internal capsule, corpus callosum and corticospinal tracts.
DWI reveals restricted diffusion in affected areas (Sener, 2002). MRS shows decreased levels of NAA and increased levels of myo-inositol and choline (Cecil & Kos, 2006).

3.2.2.2 Krabbe disease

Krabbe disease, or globoid cell leukodystrophy, is an autosomal recessive neurodegenerative disorder, caused by a deficiency of the lysosomal enzyme galactocerebrosidase, a key enzyme in metabolic pathways of myelin turnover and breakdown. Its deficiency results in galactosylsphingosine accumulation, a central and peripheral nervous system neurotoxin. The most frequent (85-90%) form of Krabbe disease has an infantile onset (Wenger, 2008). It presents with irritability between 3 and 6 months after birth and progresses with motor deterioration, feeding problems and atypical seizures. Eventually, the child develops decerebrate posture (Cecil & Kos, 2006) and dies before age 2 years. Diagnosis is made by measuring the activity of galactocerebrosidade in leukocytes or in cultured skin fibroblasts and can be confirmed by genetic studies. A molecular genetic test is available for carrier detection.
CT features during the initial stage of the disease may show symmetric high-attenuation in the thalami, caudate nuclei, corona radiate, posterior limbs of the internal capsule, brainstem and cerebellar dentate nuclei. Early in the course of the disease, MRI shows T1 and T2 prolongation in the cerebellar nuclei, posterior limbs of the internal capsules and cerebellar white matter. The subcortical U fibers are spared until late in Krabbe disease (Fig. 6.). Symmetric enlargement of the optic nerves may be seen (Cecil & Kos, 2006).
Enhancement in junction between deep white matter and subcortical U fibers is rare (Vargas et al., 2009), but may be a common feature for cranial nerves and the cauda equina (Given et al., 2001). Thalami can be normal in the early stages, or reveal decreased T1 and T2 relaxation times due to calcium deposition (Cecil & Kos, 2006). Later in the disease course, hyperintensity predominantly involves the parietal lobes, with extension to the callosal splenium, and severe, progressive atrophy.
DWI reveals restriction diffusion in the early phases of the disease, mainly in the subcortical white matter, caudate head, and anterior limb of internal capsule; in later stages it shows increased diffusion in the white matter (Engelbrecht et al., 2002). Elevated choline and myo-inositol, and reduced NAA have been found in the white matter MRS of infantile onset. Lactate elevation has also been reported (Zarifi et al., 2001). On the other hand, in an adult onset case, white matter spectrum changes were much less marked, and revealed only a mild elevation of creatine (Farina et al, 2000).

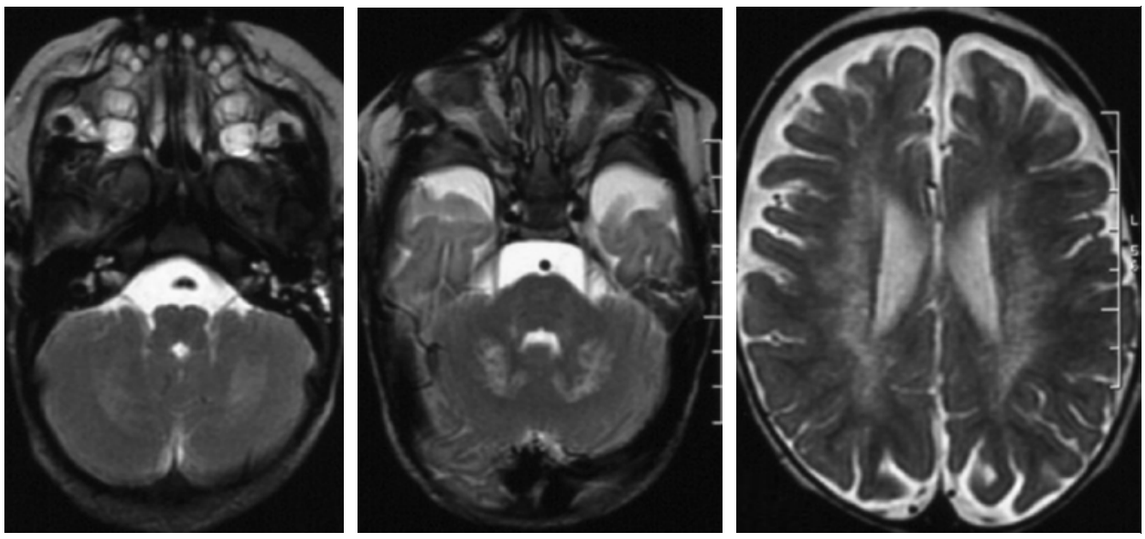

(a) (b) (c)

Fig. 6. Krabbe disease. Axial T2-WI show high signal intensity in the cerebellar white matter (a), cerebellar dentate nuclei (b), and periventricular white matter with sparing of the subcortical white matter (c).

3.2.2.3 X-linked adrenoleukodystrophy

X-linked adrenoleukodystrophy (ALD) is a peroxisomal disorder affecting the central nervous system, adrenal cortex, and testicles. It is caused by mutations in the ALD gene that encodes for a peroxisomal membrane protein. It is associated to accumulation of very long chain of fatty acids in different tissues and in plasma. Several different forms of ALD have been reported. The childhood cerebral form, the most common, with a clinical onset between ages 4 and 8 years, manifests with behavioural and school performance problems, progressive impairment of cognition, vision, hearing and motor function. Within 2 years, it leads to total disability, and to death within 5 to 8 years (Cecil & Kos, 2006). The adrenomyeloneuropathy (AMN) generally manifests in the late twenties and progresses over decades with paraparesis and sphincter and sexual dysfunction. Clinical manifestations associated to MRI features may lead to diagnosis. High concentration of very long chain fatty acids in plasma and/or cultured skin fibroblasts reinforces it. Molecular genetic testing is clinically available.

Three distinct zones have been described in white matter lesions, with direct influence in imagiologic features. An inner zone (Zone A) of astrogliosis and scarring; an intermediate zone (Zone B) of active inflammation and demyelination, with axons spared; and an outer zone (Zone C) of ongoing demyelination in absence of inflammation. A Zone D has been referred, which is peripheral to Zone C and characterized by impending demyelination (Eichler et al., 2002). In early stages, ALD CT scan and MRI have a typical appearance. Symmetric white matter changes occur predominantly in the peritrigonal regions and across the corpus callosum splenium with relative preservation of the subcortical U fibers. Spread progression occurs outwardly and cephalad as a confluent lesion, until most of the white matter is involved. CT shows symmetric low attenuation in a *butterfly* distribution, across the corpus callosum splenium, surrounded by an enhancing zone peripherally, due to inflammation. In the earliest stage, the lesion may be restricted to the splenium (Barkovich,

2005). On MRI the Zone A reveals T1 and T2 prolongation; the Zone B appears isointense on T1-WI and isointense or slightly hypointense on T2-WI, showing enhancement if paramagnetic contrast is administered; and the Zone C reveals minimally hypointense on T1-WI and hyperintense on T2-WI, without enhancement (Melhem et al., 2000). Symmetric abnormal T2 hyperintensity along the corticopontine and corticospinal tracts, and auditory pathways are common (Fig. 7.). Cases of predominantly frontal lobe involvement may occur with lesion of corpus callosum genu, anterior limbs and genu of the internal capsules, sporadically with lesion of cerebellar white matter. Atypical cases with unilateral involvement have also been reported, as well as calcifications in parieto-occipital region (Barkovich, 2005). MRI in AMN, compared to ALD, shows more frequently an involvement of cerebellar white matter and brainstem corticospinal tract and less commonly, cerebral lesion (Barkovich, 2005).

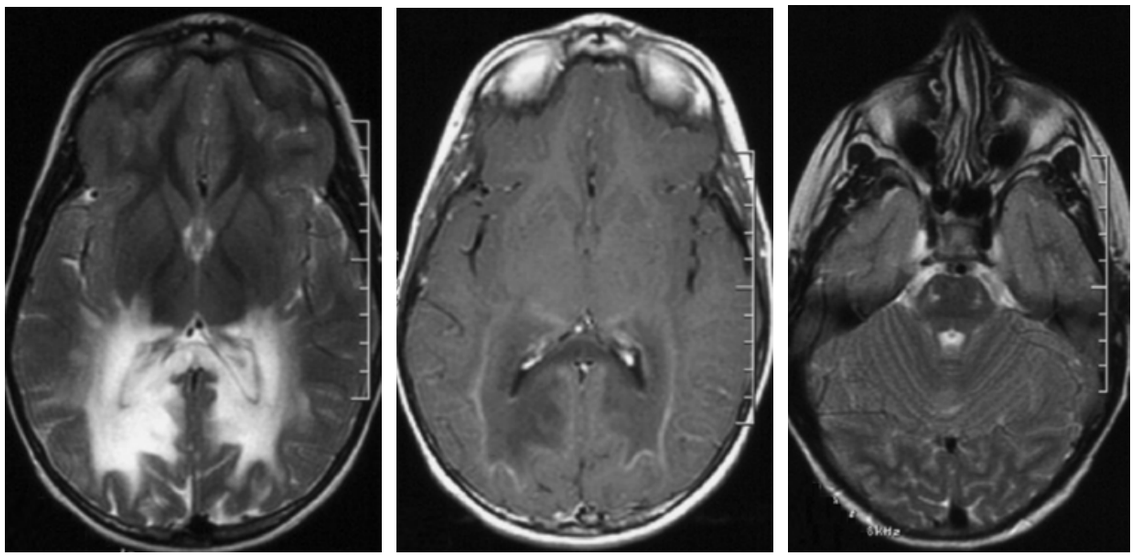

(a) (b) (c)

Fig. 7. X-linked adrenoleukodistrophy. (a) Axial T2-WI shows hyperintensity in the occipital white matter and corpus callosum splenium. (b) Axial T1-WI postcontrast shows enhancement leading edge of inflammation. (c) Axial T2-WI shows hyperintensity in the corticospinal tracts within the pons.

DWI shows an increased apparent diffusion coefficient (ADC) in Zone A (Schneider et al., 2003). MRS reveals abnormal spectrum within regions of abnormal imaging, as well as normal appearing white matter. Spectrum profile in normal appearing white matter discloses elevated choline levels. Raised choline and myo-inositol levels reflect the onset of demyelination. An increase in choline, myo-inositol and glutamine levels suggests active demyelination and glial proliferation. Decreased NAA and glutamine levels reflect neuronal loss and injury. High lactate peak is consistent with inflammation (Cecil & Kos, 2006). Detection of MRS abnormalities in asymptomatic patients or in those with stable MRI can predict disease progression.

3.2.2.4 Vanishing white matter disease

Vanishing White Matter (VWM), or childhood ataxia with central nervous system hypomyelination, is an autosomal recessive disease caused by mutation in one of the five

genes involved in eukaryotic translation initiation 2B. It may result in impairment of the ability of cells to regulate protein synthesis in response to stress (Pronk et al., 2006). Its phenotype varies widely from antenatal onset with early death, to adult onset with slowly progressive disease. In late onset cases, motor and mental development is normally or mildly delayed at first. Chronic progressive or subacute neurological deterioration, with cerebellar ataxia, spasticity, and variable optic atrophy frequently occurs between the ages of 2 and 6 years. Epilepsy is not a major sign of the disease, and, unlike motor abilities, mental capacities are relatively preserved. Episodes of rapid deterioration can occur after minor trauma or infection, ending in unexpected coma. Death happens a few years after onset (van der Knaap et al., 1998). Diagnosis is based on clinical manifestations, MRI features, and mutation identification in one of the five mentioned genes (Schiffmann et al., 2010).

CT scan reveals symmetric and diffuse white matter low density in the cerebral hemispheres. MRI is typical, showing symmetric and diffuse white matter anomalies. Subcortical involvement occurs during early stages of disease, with swelling and enlargement of gyri. On the later stages, white matter reveals signal intensity which is close to, or similar to cerebrospinal fluid in every sequence (Fig. 8.). On FLAIR and T1-WI there is a radiating, stripe-like pattern, on sagittal and coronal images; and a dot-like pattern in the centrum semiovale, on the axial images, which corresponds to remain tissue strands. Overtime, cystic lesions develop. Cerebellar atrophy may be seen, mainly involving the vermis. Dorsal pons hyperintensity is seen at the beginning; in later stages, involvement of the ventral pons also occurs (van der Knaap et al., 2006).

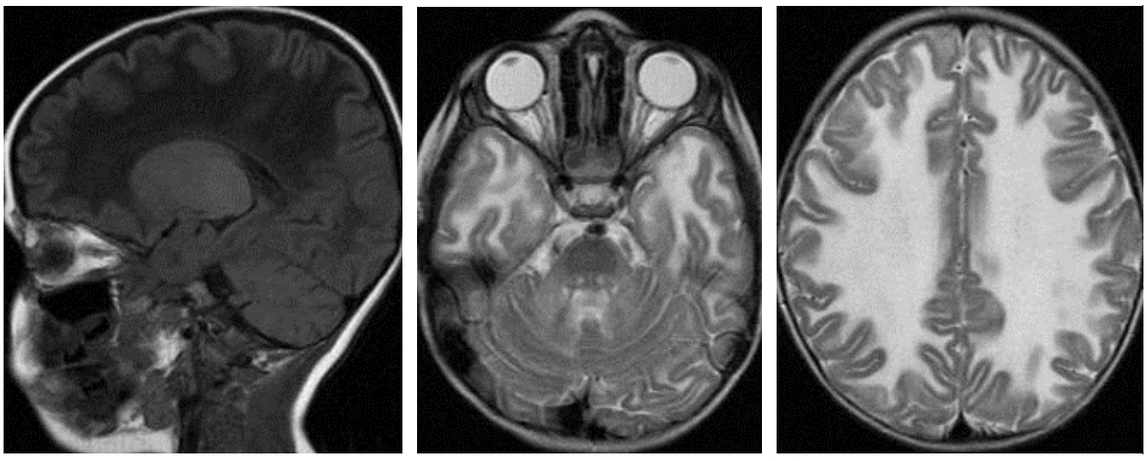

(a) (b) (c)

Fig. 8. Vanishing white matter disease. (a) Sagittal T1-WI shows abnormal cerebral white matter hypointensity. T2-WI shows hyperintensity involving central tegmental tract in the dorsal pons (b) and cerebral white matter (c).

MRS in the white matter shows marked decrease in NAA, creatine and choline peaks, or even virtual absence of all parenchymal metabolites, with presence of lactate and glucose. Gray matter spectrum is nearly normal, with a small increase in lactate and glucose, and a decrease in NAA peaks (van der Knaap et al., 1998).

4. Disorders involving both gray and white matter

When the damage affects the gray matter and white matter, it is important to recognize if the lesions involve deep gray matter, or if, in addition to the white matter, the cortical gray matter is the only one to be affected (Barkovich, 2005, 2007).

4.1 Disorders involving white matter and cortical gray matter

This group of IEM includes peroxisomal disorders such as Zellweger syndrome, Alpers disease, Menkes disease, mucopolysaccharidoses and mucolipidoses (Barkovich, 2005).

4.2 Disorders involving white matter and deep gray matter

The list of IEM with white matter and deep gray matter involvement is wide, but the identification of the nuclei that is early affected can help narrowing the differential diagnosis. The involvement of thalami is present in GM1 and GM2 gangliosidoses, Krabbe disease, and Wilson's disease. The lesion of globi pallidi is present in Canavan disease, methylmalonic acidemia, MSUD, Kearns-Sayre syndrome, L-2-hydroxyglutaric aciduria, and urea cycle disorders (Barkovich, 2005). When the involvement is seen in striata, the differential diagnosis should include glutaric aciduria type I, propionic acidemia, ethylmalonic acidemia, Wilson's disease, MELAS and Leigh syndrome.

4.2.1 Canavan disease

Canavan disease, or spongiform leukodystrophy, is an autosomal recessive disorder, characterized by deficiency of N-acetylaspartylase resulting in abnormal accumulation of N-acetylaspartic acid. Three clinical forms - neonatal, infantile, and late onset - are recognized (Traeger & Rapin, 1998). Most commonly, Canavan disease presents within the first 6 months of life with hypotonia, lack of head control, macrocephaly, irritability and development delay. Later on, spasticity, optic atrophy and seizures ensue (Cecil & Kos, 2006). Death occurs within the teens. Suspicion of diagnosis is based on clinical manifestation and MRI features. Diagnosis is confirmed by demonstration of high concentration of N-acetylaspartic acid in the urine. Molecular genetic testing is clinically available (Matalon & Bhatia, 2009).

CT scan shows diffuse hypodensity in the cerebral and cerebellar white matter (Barkovich, 2005). MRI shows symmetric areas of diffuse confluent white matter areas of T1 and T2 prolongation. The subcortical U fibers are preferentially affected in the beginning of the disease. Globi pallidi are frequently involved, as well as thalami. In some cases internal and external capsules (Cheon et al, 2002), cerebellar white matter and brain stem can also be affected (Matalon & Bhatia, 2009). In the later stages, there is a diffuse atrophy of white matter.

MRS in white matter shows marked elevation of the NAA peak, which is classically assumed to be exclusive for Canavan disease, although it can also be seen some times in Salla disease and PMD (Varho et al, 1999).

4.2.2 Maple syrup urine disease

Maple syrup urine disease (MSUD), an autosomal recessive disorder, is caused by deficiency of the branched-chain alpha-ketoacid dehydrogenase (BCKAD) complex, leading to accumulation of the branched-chain amino acids (BCAAs), allo-isoleucine and branched-

chain ketoacids (BCKAs) in tissues and plasma (Strauss et al., 2009). MSUD manifests as heterogeneous clinical and molecular phenotypes. Several clinical forms have been described with manifestations from early acute neonatal to chronic intermittent forms diagnosed in adolescents. Classic MSUD causes maple syrup odor in urine and cerumen, soon after birth. At age 2-3 days newborns present with irritability, poor feeding and ketonuria. At age 4-5 days lethargy, apneia, opisthotonus and stereotyped movements occur; followed by coma and central respiratory failure at age 7-10 days. High protein ingestion or any cause of enhanced catabolism like infection, injury or surgery, can lead to acute leucine intoxication with cerebral oedema and neurological impairment (Morton et al., 2002). In less severe cases, patients reveal normal or moderately retarded neurodevelopment, later presenting with metabolic crises similar to classic MSUD. Suspicion of diagnosis, based on clinical manifestations (and eventually MRI features in late onset cases), can be confirmed by elevation of BCAAs, allo-isoleucine and BCKAs in tissues and plasma. Molecular genetic testing is also clinically available (Strauss et al., 2009). In Portugal, extended newborn screening detects MSUD, frequently in a pre-symptomatic stage.

Cranial ultrasonography can be useful in symptomatic neonates, showing symmetric hyperechogenicity of periventricular white matter, basal ganglia (mainly globi pallidi) and thalami (Fariello et al., 1996).

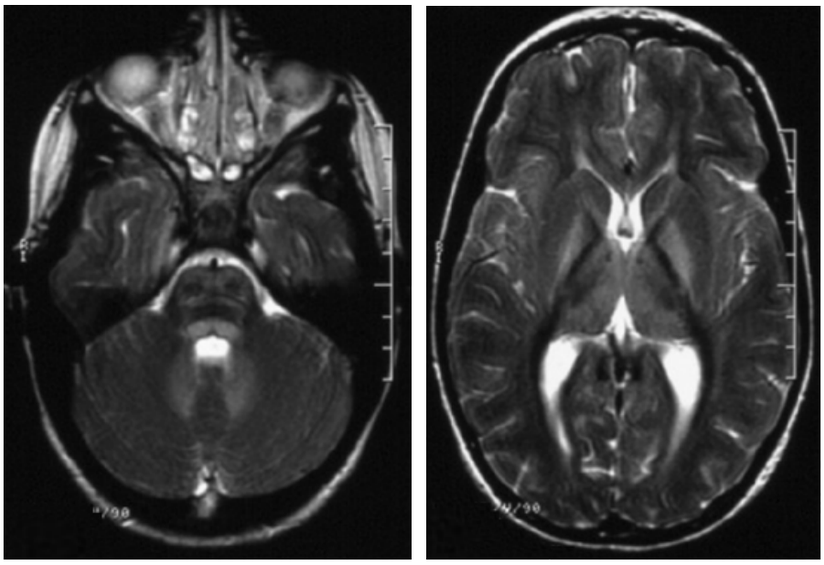

(a) (b)

Fig. 9. Maple syrup urine disease. Axial T2-WI show hyperintensity in the brainstem and cerebellar white matter (a), globus pallidi and thalami (b).

Acute classic MSUD form shows signs of diffuse oedema, characterized by hypodensity on CT scan, and T1 and T2 prolongation on MRI. Severe localized oedema (MSUD oedema) is seen in myelinated areas at birth, namely deep cerebellar white matter, posterior brain stem, cerebral peduncles, thalami, posterior limb of internal capsule, posterior centrum semiovale, and globi pallidi (Fig. 9.) (Brismar et al., 1990). Forms with later onset reveal lack of myelination superimposed upon lesions located at the same regions affected by MSUD

oedema in acute classic form. Brain sequel depends on the time it takes to reverse metabolic decompensation (Barkovich, 2005).
DWI is very important, as the oedema may be hard to identify in T2-WI due to nonmyelinated brain hyperintensity. Regions with acute MSUD oedema show restricted diffusion with decreased ADC value. Diffusion-tensor imaging (DTI) reveals decreased anisotropy in the same areas (Parmar et al., 2004). In acute phase, MRS with long TE reveals elevated levels of lactate and presence of an abnormal BCAAs and BCKAs peak at 0.9 ppm. These changes can reverse completely after metabolic correction (Jan et al., 2003).

4.2.3 L-2-hydroxyglutaric aciduria

L-2-hydroxyglutaric aciduria is an autosomal recessive disease caused by mutations in L-2-hydroxyglutarate dehydrogenase gene, with accumulation of L-2-hydroxyglutac acid in urine, cerebrospinal fluid and plasma. It is characterized by slowly progressive neurological dysfunction with cerebellar ataxia, psychomotor retardation, seizures, macrocephaly, and extrapyramidal and pyramidal signs (Steenweg et al., 2010). It presents in childhood, frequently after a period of normal psychomotor development. Diagnosis is suggested by typical MRI features and by measurement of L-2-hydroxyglutaric acid in urine, cerebrospinal fluid or serum. Molecular genetic testing is clinically available (Seashore, 2009).

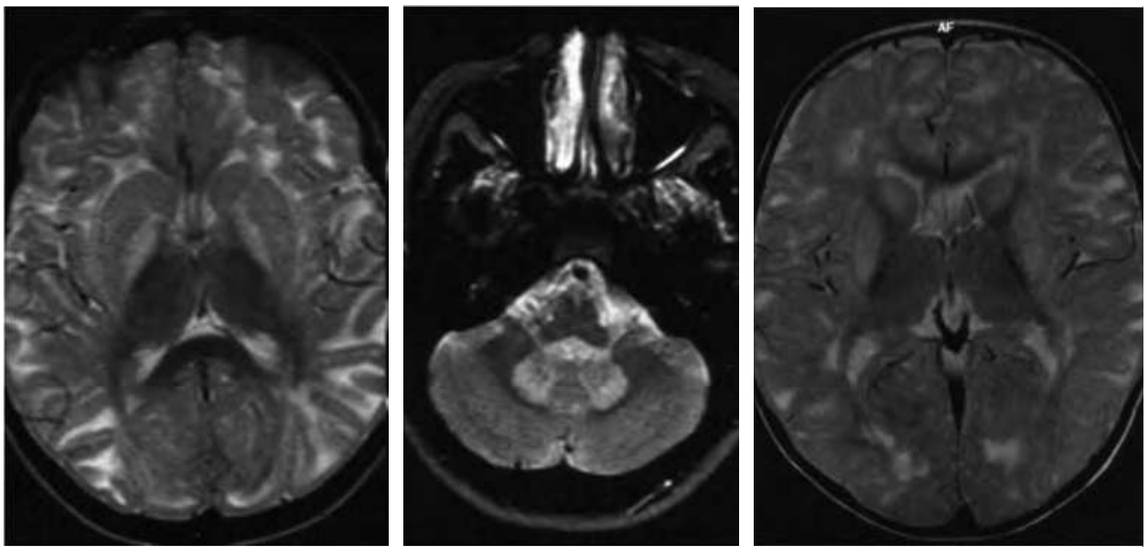

(a) (b) (c)

Fig. 10. L-2-hydroxyglutaric aciduria. Axial T2-WI show hyperintensity of the subcortical WM and globus pallidi (a), dentate nuclei (b), putamina and caudate nuclei (c).

CT scan shows symmetrical hypodensity in subcortical white matter, globi pallidi, and frequently dentate nuclei (Topçu et al., 1996). MRI reveals hyperintensity in the same locations listed above, with a preferential involvement of the frontal over the occipital white matter. The periventricular white matter is spared, as well as internal capsule, corpus callosum, cerebellar white matter, and brainstem. Sometimes involvement of putamina and caudate nuclei are seen (Fig. 10.). Globi pallidi, and sometimes cerebellar vermis and

hemisphere, reveal atrophy. Swelling of the cerebral white matter with broadening of gyri, rarefaction of the subcortical white matter and atrophy of cerebral white matter were also reported (Steenweg et al., 2009).
DWI shows increased diffusion in the white matter lesions. MRS is usually normal, but it can reveal a slight decrease of NAA peak, in short TE (Aydin et al, 2003).

4.2.4 Glutaric aciduria type I

Glutaric aciduria type I is an autosomal recessive disorder resulting from a deficiency in glutaryl-CoA dehydrogenase with accumulation of glutaric, 3-hydroxyglutaric and glutaconic acids and secondary carnitine deficiency. Typically the disorder presents with an acute encephalopathy between 6 and 18 months of age, in a previously healthy or mildly motor retarded, macrocephalic child. In some cases, a slowly progressive course with mental retardation, hypotonia, dystonia, choreoathetosis, spastic quadriplegia and macrocephaly is seen (Hoffmann & Zschocke, 1999). Diagnosis is suggested by classical MRI features that are highly typical, and made by measurement of glutaric, 3-hydroxyglutaric and glutaconic acids in urine. Molecular genetic testing is clinically available (Seashore, 2009). In Portugal, broad neonatal screening detects glutaric aciduria type I in a pre-symptomatic phase.
CT scan shows diffuse white matter hypodensity and/or cerebral atrophy, most prominent in the frontal and temporal regions (Yager et al., 1988). MRI reveals symmetric widening of the Sylvian fissure, frontotemporal volume loss, and delayed myelination. Putamen T2 hyperintensity is predominantly seen, either alone or in combination with the caudate nucleus. Globus pallidus is less affected. Later in the course of disease, periventricular white matter T2 hyperintensity, basal ganglia and cerebral atrophy are seen. Sometimes imagiological studies reveal acute or chronic subdural haematomas (Fig. 11.), implying differential diagnosis with nonaccidental trauma (Neumaier-Probst et al., 2004).

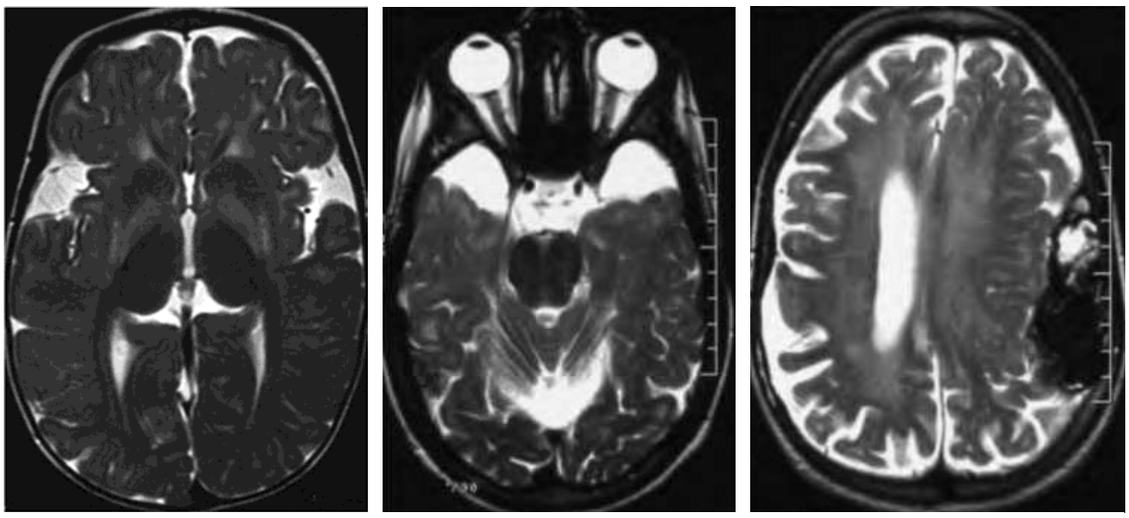

(a) (b) (c)

Fig. 11. Glutaric aciduria type I. Axial T2-WI show putamina and globi pallidi hyperintensity (a), expansion of pericerebral fluid spaces anterior to the temporal lobes (b), periventricular white matter hyperintensity, cerebral atrophy and left frontoparietal subdural hematoma (c).

DWI shows restricted diffusion in acute basal ganglia lesions. MRS shows decreased NAA/creatine ratio at the basal ganglia in encephalopathic patients (Pérez-Dueñas at al., 2009).
Fluoro-2-deoxyglucose PET reveals decreased glucose uptake in the cerebral cortex, basal ganglia and thalami (Al-Essa et al., 1998).

4.2.5 Mitochondrial encephalomyopathy with lactic acidosis and stroke-like episodes (MELAS)

MELAS is a multisystem mitochondrial disorder, with early normal psychomotor development and onset typically between the ages 2 and 10 years. It is characterised by neurological manifestations including seizures, encephalopathy, recurrent headaches and stroke-like episodes (hemiparesis and hemianopsia). Diagnosis is based on an association of clinical findings, MRI features and molecular genetic testing. Mitochondrial DNA mutation A3243G is found in 80% of MELAS patients. Sometimes, pathogenic mutations may be undetectable in mtDNA from leukocytes, and it is necessary to resort to other tissues, such as skeletal muscle, which is the most reliable for diagnosis (DiMauro & Hirano, 2010).
Stroke-like lesions are often transient, affecting mainly the gray matter and are not restricted to specific vascular territories, unlike embolic and thrombotic infarction (Barkovick, 2005). They are usually fluctuating. Acute ischemic episodes show swelling and hypodensity on CT scan, and T1 and T2 prolongation on MRI, commonly involving the temporo-parieto-occipital lobes and basal ganglia (Fig. 12.).
With regard to DWI findings, reports are discordant. Some early reports demonstrate an increased diffusion in stroke-like lesions. However the number of reports revealing a decreased diffusion in these areas has increased. Thus, the absence of vasogenic oedema should not weaken the possibility of MELAS in favour of ischemic stroke. MRS shows a decrease in NAA and an increase in lactate in stroke-like lesions (Fig. 12.) (Tzoulis & Bindoff, 2009). An increase in lactate is also seen in embolic and thrombotic infarction, so this finding is not specific of MELAS.

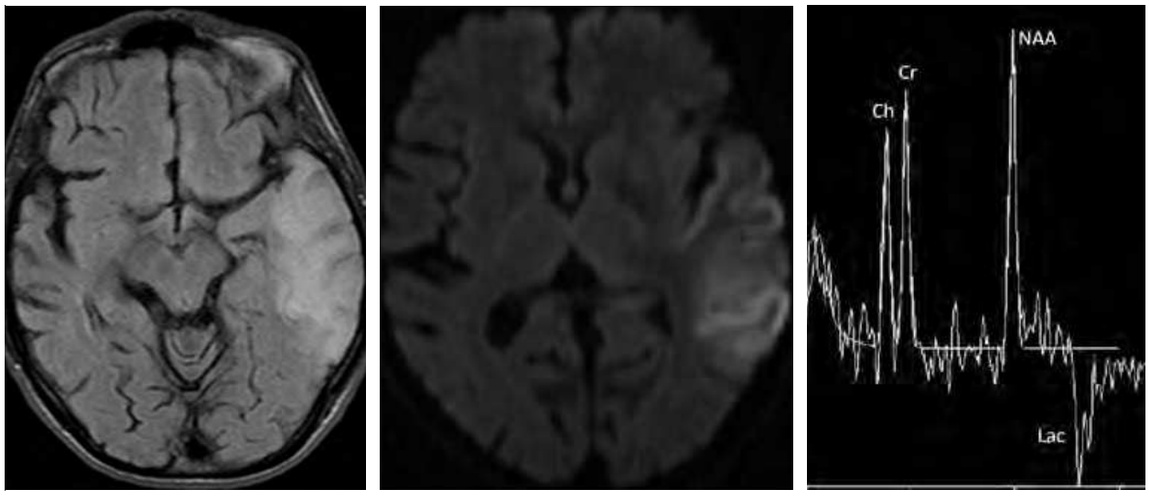

(a) (b) (c)

Fig. 12. MELAS. (a) Axial FLAIR shows hyperintensity in left temporal lobe. (b) Axial DWI (b=1000) shows restriction diffusion of the lesion. (c) Single voxel proton MRS (TE = 135 ms) of the lesion shows a lactate doublet (Lac). (This case is a courtesy of Dr. Fernando Matias)

SPECT shows hyperperfusion in the acute stage of stroke-like episodes, and hypoperfusion in the chronic stage (Tzoulis & Bindoff, 2009). PET and xenon reveal increased blood flow and decreased glucose uptake and oxygen extraction fraction in the lesion areas (Barkovich, 2005).

4.2.6 Leigh syndrome

Leigh syndrome, or subacute necrotizing encephalomyelopathy, is caused, in the majority of the cases, by a dysfunction of the mitochondrial respiratory chain (particularly complexes I, II, IV or V), the coenzyme Q, or the pyruvate dehydrogenase complex (Finsterer, 2008). Most children are normal at birth and manifested usually by the end of the first year of life. The onset is commonly insidious, and the course may be intermittently progressive for some years. Clinical presentation can be highly variable, and includes psychomotor retardation, feeding difficulties, recurrent episodes of vomiting, failure thrive, signs of brainstem, cerebellar and basal ganglia dysfunction, and lactic acidosis (Medina et al., 1990). Diagnosis is suggested by clinical criteria and MRI features. Molecular genetic testing allows for a specific etiological diagnosis.

Neuroradiological findings in Leigh syndrome are symmetrical hypodensities on CT, and T1 and T2 prolongation on MRI, in the basal ganglia and thalami. Lesions can involve the substantia nigra, periaqueductal gray matter within the midbrain, inferior colliculus, inferior olivary nuclei, inferior cerebellar peduncles, medulla, solitary tract in the medulla, central tegmental tract and reticular formation in the dorsal pons (Barkovich 2005). Less commonly, the red nuclei and cerebellar dentate nuclei are involved. Basal ganglia are often affected before the brainstem, but in some patients, brainstem lesions appear without basal ganglia alterations (Fig. 13.). Sometimes, MRI reveals delayed myelination. In most patients,

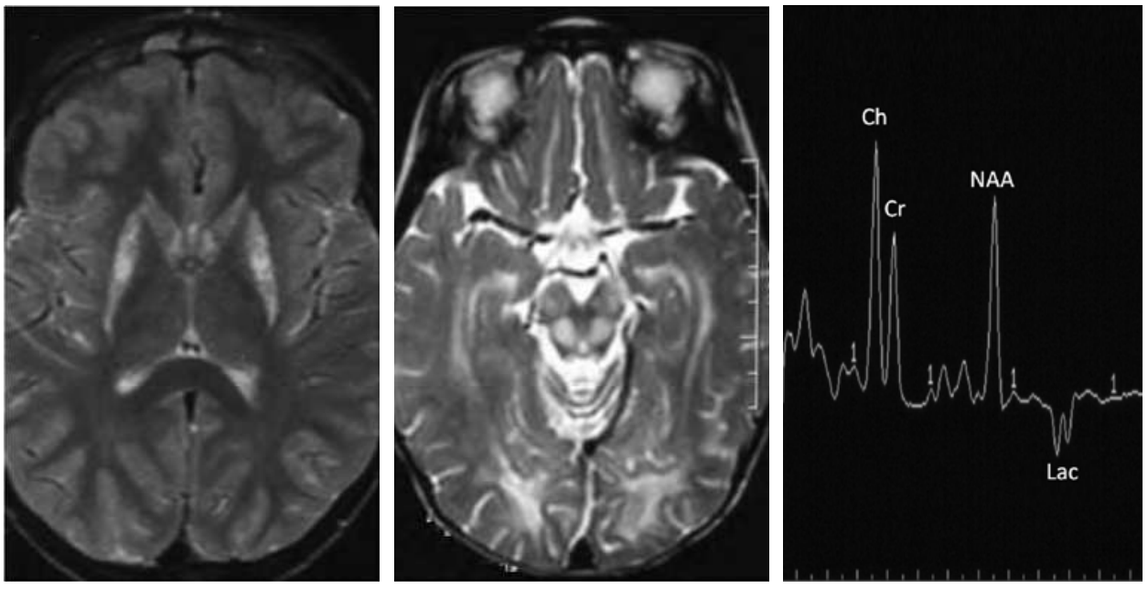

(a) (b) (c)

Fig. 13. Leigh syndrome. Axial T2-WI show hyperintensity in the striata (a), dorsal midbrain and cerebral peduncles (b). (c) Multivoxel proton MRS (TE = 144 ms) of the basal ganglia shows a decreased of NAA peak and a lactate doublet (Lac).

cerebral white matter is generally involved in the later stages of disease (Arii & Tanabe, 2000). In some cases, a marked global atrophy can be seen, over time. Some MRI patterns may suggest an implicated mutation. In SURF-1 mutation, associated to complex IV deficiency, basal ganglia are less involved, and the brainstem, subthalamic nuclei, cerebellar nuclei and cerebellar peduncles are commonly involved. ATPase 6 mutation, which is associated to maternally inherited Leigh syndrome (MILS), shows anterior putamina, globi pallidi and dorsal mesencephalon and pons lesions. In the absence of hypoxia, ischemia or infection, symmetric involvement of deep gray matter is very suspicious of a mitochondrial defect (Saneto et al., 2008).

DWI shows reduced diffusion in acute lesions and increased diffusion in chronic ones. MRS reveals increase in lactate and a small decrease of NAA in lesions, and alongside the imagiological features of conventional MR it supports the diagnosis of Leigh syndrome (Barkovich, 2005).

5. Conclusion

MRI plays an essential role in the diagnosis of IEM. It shows high sensitivity in the detection of some of these disorders and evaluation of their severity. Despite of the nonspecificity of many features, a systematic pattern recognition approach to brain structures involved is useful, as it narrows differential diagnosis. MRS can help in this process and may disclose anomalies, even if there are no lesions detectable with conventional MRI. Further investigation and accurate characterization of neuroradiological features are needed in order to gather a wider range of specific patterns. These would allow more patients to be adequately classified.

6. References

Al-Essa, M. e tal.. (1998). Fluro-2-deoxyglucose (18FDG) PET scan of the brain in glutaric aciduria type I: clinical and MRI correlations. *Brain Dev*, Vol.20, No.5, (August 1998), pp. 295-301, ISSN 0387-7604

Arii, J. & Tanabe, Y. (2000). Leigh syndrome: serial MR imaging and clinical follow-up. *Am J Neuroradiol*, Vol.21, No.8, (September 2000), pp. 1502-1509, ISSN 0195-6108

Autti, T. et al.. (1996). MRI of neuronal ceroid lipofuscinosis. I. Cranial MRI of 30 patients with juvenile neuronal ceroid lipofuscinosis. *Neuroradiology*, Vol.38, No.5, (July 1996), pp. 476-482, ISSN 0028-3940

Aydin, K. et al.. (2003). Single-voxel MR spectroscopy and diffusion-weighted MRI in two patients with L-2-hydroxyglutaric aciduria. *Pediatr Radiol*, Vol.33, No.12, (December 2003), pp. 872-876, ISSN 0301-0449

Barkovich, A. (2005). *Pediatric Neuroimaging* (4th edition) Lippincott Williams & Wilkins, ISBN 0-7817-5766-5, Philadelphia

Barkovich, A. (2006). A magnetic resonance approach to metabolic disorders in childhood. *Rev Neurol*, Vol.10, No.43, (October 2006), pp. 5-16, ISSN 0210-0010

Barkovich, A. (2007). An approach to MRI of metabolic disorders in children. *Journal of neuroradiology*, Vol.34, (2007), pp. 75-88, ISSN 0195-6108

Boor, I. et al.. (2007). MLC1 is associated with the dystrophin-glycoprotein complex at astrocytic endfeet. *Acta Neuropathol*. Vol.114, No.4, (October 2007), pp. 403-410, ISSN 0001-6322

Brismar, J. et al.. Maple syrup urine disease: findings on CT and MR scans of the brain in 1o infants. *Am J Neuroradiol*, Vol.11, No.6, (November-December 1990), pp. 1219-1228, ISSN 0195-6108

Brokmann, K. et al.. (1996). Localized proton magnetic resonance spectroscopy of cerebral metabolic disturbances in children with neuronal ceroid lipofuscinosis. *Neuropediatrics*, Vol.27, No.5, (October 1996), pp. 242-248, ISSN 1439-1899

Campistol, J. (1999). Aproximación al diagnostic de los errors congénitos del metabolismo por la neuroimagen. *Rev Neurol*, Vol.28, No.161, (1999), pp. 16-23, ISSN 1576-6578

Cecil, K. & Kos, R. (2006). Magnetic resonance spectroscopy and metabolic imaging in white matter diseases and pediatric disorders. *Top Magn Reson Imaging*, Vol.17, No.4, (August 2006), pp. 275-293, ISSN 1536-1004

Cheon, J. et al.. (2002). Leukodystrophy in children: a pictorial review of MR imaging features. *Radiographics*, Vol.22, No.3, (May-June 2002), pp. 461-476, ISSN 0271-5333

Chilosi, A. et al.. (2008). Treatment with L-arginine improves neuropsychological disorders in a child with creatine transporter defect. *Neurocase*, Vol.14, No.2, (2008),pp. 151-161, ISSN 1465-3656

DiMauro, S. & Hirano, M. (October 2010). MELAS, In: GeneReviews, 03.02.2011, Available from http://www.ncbi.nlm.nih.gov/books/NBK1233/#melas.Summary

Dyke, J. et al.. (2007). Assessing disease severity in late infantile neuronal ceroid lipofuscinosis using quantitative MR diffusion-weighted imaging. *Am J Neuroradiol*, Vol.28, (August 2007), pp. 1232-1236, ISSN 0195-6108

Eichler, F. et al.. (2002). Proton MR spectroscopy and diffusion tensor brain MR imaging in X-linked adrenoleukodystrophy: initial experience. *Radiology*, Vol.225, No.1, (October 2002), pp. 245-252, ISSN 0033-8419

Engelbrecht, V. et al.. (2002). Diffusion-weight MR imaging in the brain in children: findings in the normal brain and in the brain with white matter diseases. *Radiology*, Vol.222, No.2, (February 2002), pp. 410-418, ISSN 0033-8419

Fariello, G. et al.. (1996). Cranial ultrasonography in maple syrup urine disease. Am J *Neuroradiol*, Vol.17, No.2, (February 1996), pp. 311-315, ISSN 0195-6108

Farina, L. et al.. (2000). MR imaging and proton MR spectroscopy in adult Krabbe disease. *Am J Neuroradiol*, Vol.21, No.8, (September 2000), pp. 1478-1482, ISSN 0195-6108

Finsterer, J. (2008). Leigh and leigh-like syndrome in children and adults. *Pediatr Neurol*, Vol.39, No.4, (October 2008), pp. 223-235, ISSN 0887-8994

Fluharty, A. (September 2008). Arysulfatase A deficiency. In: GeneReviews, 24.02.2011, Available from http://www.ncbi.nlm.nih.gov/books/NBK1130/#mld.Summary

Gelal, F. et al.. (2002). van der Knaap's leukoencephalopathy: report of five new cases with emphasis on diffusion-weighted MRI findings. *Neuroradiology*, Vol.44, No.7, (July 2002), pp. 625-630, ISSN 0028-3940

Given, C. et al.. (2001). Intracranial and spinal MR imaging findings associated with Krabbe's disease: case report. *Am J Neuroradiol*, Vol.22, No.9, (October 2001), pp. 1782-1785, ISSN 0195-6108

Gorospe, J. (April 2010). Alexander disease, In: GeneReviews, 28.02.2011, Available from http://www.ncbi.nlm.nih.gov/books/NBK1172/

Haltia, M. (2003). The neuronal ceroid-lipofuscinoses. *J Neuropathol Exp Neurol*, Vol.62, No.1, (January 2003), pp. 1-13, ISSN 0022-3069

Hanefeld, F. et al.. (2005). Quantitative proton MRS of Pelizaeus-Merzbacher disease: evidence of dys- and hypomyelination. *Neurology*, Vol.65, No.5, (September 2005), pp.701-706, ISSN 0028-3878

Hayflick, S. et al.. (2003). Genetic, clinical and radiographic delineation of Hallervorden-Spatz syndrome. *N Engl J Med*, Vol.348, No.1, (January 2003), pp. 33-40, ISSN 0028-4793

Hayflick, S. et al.. (2006). Brain MRI in neurodegeneration with brain iron accumulation with and without PANK2 mutations. *Am J Neuroradiol*. Vol.27, No.6. (June-July 2006), pp.1230-1233, ISSN 0195-6108

Hoffmann, G. & Zschocke, J. (1999). Glutaric aciduria type I: from clinical, biochemical and molecular diversity to successful therapy. *J Inherit Metab Dis*, Vol.22, No.4, (June 1999), pp. 381-391, ISSN 0141-8955

Incerti, L. (2000). MRI in neuronal ceroid lipofuscinosis. *Neuro Sci*, Vol.21, No.1, (2000), pp. 71-73, ISSN 1590-1874

Jan, W. et al.. (2003) MR diffusion imaging and MR spectroscopy of maple syrup urine disease during acute metabolic decompensation. *Neuroradiology*, Vol.45, No.6, (June 2003), pp. 393-399, ISSN 0028-3940

Järvelä, I. et. al.. (1997). Clinical and magnetic resonance imaging findings in Batter disease: analysis of the major mutation (1.02-kb deletion). *Ann Neurol*, Vol.42, No.5, (1997), pp. 799-802, ISSN 0364-5134

Kiriyama, T. et al.. (2007). SPECT revealed cortical dysfunction in a patient ho had genetically definite megalencephalic leukoencephalopathy with subcortical cysts. *Clin Neurol Neurosurg*, Vol.109, No.6, (July 2007), pp. 526-530, ISSN 0303-8467

Matalon, R. & Bhatia, G. (October 2009). Canvan disease, In: GeneReviews, 02.03.2011, Available from http://www.ncbi.nlm.nih.gov/books/NBK1234/

Medina, L. et al.. (1990). MR findings in patients with subacute necrotizing encephalomyelopathy (Leigh syndrome): correlation with biochemical defect. *Am J Neuroradiol*, Vol.11, No.2, (March-April 1990), pp. 379-384, ISSN 0195-6108

Melhem, E. et al.. X-linked adrenoleukodystrophy: the role of contrast-enhanced MR imaging in predicting disease progression. *Am J Neuroradiol*, Vol.21, No.5, (May 2000), pp. 839-844, ISSN 0195-6108

Mercimek-Mahmutoglu, S. & Stöckler-Ipsiroglu, S. (January 2009). Creatine deficiency syndromes, In: GeneReviews, 21.02.2011, Available from http://www.ncbi.nlm.nih.gov/books/NBK3794/#creatine.Clinical_Description

Mercimek-Mahmutoglu, S. et al.. (2010). Treatment of intractable epilepsy in a femalewith SLC6A8 deficiency. *Mol Genet Metab*, Vol.101, No.4, (December 2010), pp. 409-412, ISSN 1096-7192

Morita, H. et al.. (2006). MR imaging and 1H-MR spectroscopy of a case of van der Knaap disease. *Brain Dev*, Vol.28, No.7, (August 2006), pp. 466-469, ISSN 0387-7604

Morton, D. et al.. (2002). Diagnosis and treatment of maple syrup disease: a study of 36 patients. *Pediatrics*, Vol.109, No.6, (June 2002), pp. 999-1008, ISSN 0031-4005

Neumaier-Probst, E. et al.. (2004). Neuroradiological findings in glutaric aciduria type I (glutaryl-CoA dehydrogenase deficiency). Vol.27, No.6, (2004), pp. 869-876, ISSN 0141-8955

Parashari, U. et al.. (2010). Case report: MR spectroscopy in pantothenate kinase-2 associated neurodegeneration. *Indian J Radiol Imaging*, Vol.20, No.3, (August 2010), pp. 188-191, ISSN 0971-3026

Parmar, H. et al.. (2004). Maple syrup urine disease: diffusion-weighted and diffusion-tensor magnetic resonance imaging findings. *J Comput Assist Tomogr*, Vol.28, No.1, (January-February 2004), pp. 93-97, ISSN 0363-8715

Pérez-Dueñas, B. et al.. (2009). Brain injury in glutaric aciduria type I: the value of functional techniques in magnetic resonance imaging. *Eur J Paediatric Neurol*, Vol.13, No.6, (November 2009), pp. 534-540, ISSN 1090-3798

Pizzini, F. et al.. (2003). Proton MR spectroscopy imaging in Pelizaeus-Merzbacher disease. *Am J Neuroradiol*, Vol.24, No.8, pp.1683-1689, ISSN 0195-6108

Plecko, B. et al.. (2003). Degree of hypomyelination and magnetic resonance spectroscopy findings in patients with Pelizaeus Merzbacher phenotype. *Neuropediatrics*, Vol.34, No.3, (June 2003), pp.127-136, ISSN 1439-1899

Póo-Arqüelles, P. et al.. (2006). X-linked creatine transporter deficiency in two patients with severe mental retardation and autism. *J Inherit Metab Dis*, Vol.29, No.1, (February 2006), pp. 220-223, ISSN 1573-2665

Pronk, J. et al.. (2006). Vanishing white matter disease: a review with focus on its genetics. *Ment Retard Dev Disabil Res Rev*, Vol.12, No.2, (2006), pp.123-128, ISSN 1080-4013

Raghuveer, T. et al.. (2006). Inborn errors of metabolism in infancy and early childhood: an update. *Am Fam Physician*, Vol.73, No.11, (June 2006), pp. 1981-90, ISSN 0002-838X

Saneto, R. et al.. (2008). Neuroimaging of mitochondrial disease. *Mitochondrion*, Vol.8, No.5-6, (December 2008), pp. 396-413, ISSN 1567-7249

Schiffmann, R. et al.. (February 2010). Childhood ataxia with central nervous system hypomyelination/vanishing white matter, In: GeneReviews, 27.02.2011, Available from http://www.ncbi.nlm.nih.gov/books/NBK1258/

Schneider, J. et al.. (2003). Diffusion tensor imaging in cases of adrenoleukodystrophy: preliminary experience as a marker for early demyelination? *Am J Neuroradiol*, Vol.24, No.5, (May 2003), pp. 819-824, ISSN 0195-6108

Schulze, A. (2003). Creatine deficiency syndromes. *Mol Cell Biochem*, Vol.244, No.1-2, (February 2003), pp. 143-150, ISSN 0330-8177

Scriver, C. et al.. (2001). *The metabolic and molecular basis of inherited diseases*, ISBN 9780079130358, New York

Seashore, M. (December 2009). The organic acidemias: an overview, In: GeneReviews, 03.03.2011, Available from http://www.ncbi.nlm.nih.gov/books/NBK1134/

Sener, R. (2002). Metachromatic leukodystrophy: diffusion MR imaging findings. *Am J Neuroradiol*, Vol.23, No.8, (September 2002), pp. 1424-1426, ISSN 0195-6108

Steenweg, M. et al.. (2009) L-2-hydroxyglutaric aciduria: pattern of MR imaging abnormalities in 56 patients. *Radiology*, Vol.251, No.3, (June 2009), pp. 856-865, ISSN 0033-8419

Steenweg, M. et al.. (2010). An overview of L-2-hydroxyglutarate dehydrogenase gene (L"HGDH) variants: a genotype-phenotype study. *Hum Mutat*, Vol.31, No.4, (April 2010), pp. 380-390, ISSN 1059-7794

Strauss, K. et al.. (December 2009). Maple syrup urine disease, In: GeneReviews, 27.02.2011, Available from http://www.ncbi.nlm.nih.gov/pubmed/20301495

Traeger, E. & Rapin, I. (1998). The clinical course of Canavan disease. *Pediatric Neurol*, Vol.18, No.3, (March 1998), pp. 207-212, ISSN 0887-8994

Topçu, M. et al.. (2009). Clinical and magnetic resonance imaging features of L-2-hydroxyglutaric acidemia: report of three cases in comparison with Canavan disease. *J Child Neurol*, Vol.11, No.5, (September 1996), pp. 373-377, ISSN 0883-0738

Tzoulis, C. & Bindoff, L. (2009). Serial diffusion imaging in a case of mitochondrial encephalomyopathy, lactic acidosis, and stroke-like episodes. *Stroke*, Vol.40, No.2, (February 2009), pp. 15-17, ISSN 0039-2499

van der Knaap, M. & Valk, J. (1989). The reflection of histology in MR imaging of Pelizaeus-Merzbacher disease. *Am J Neuroradiol*, Vol.10, No.1, (January-February 1989), pp. 99-103, ISSN 0195-6108

van der Knaap, M. et al. (1995). Leukoencephalopathy with swelling and a discrepantly mild clinical course in eight children. *Ann Neurol*, Vol.37, No.3, (March 1995), pp. 324-334, ISSN 0364-5134

van der Knaap, M. et al.. (1998). Phenotypic variation in leukoencephalopathy with vanishing white matter. *Neurology*, Vol.51, No.2, (August 1998), pp. 540-547, ISSN 0028-3878

van der Knaap, M. et al.. (2001). Alexander disease: diagnosis with MR imaging. *Am J Neuroradiol*, Vol.6, No.4, (March 2001), pp.541-552, ISSN 0195-6108

van der Knaap, M. & Valk, J. (2005). *Magnetic resonance of myelin, myelination and myelin disorders* (3rd edition), Springer, ISBN 978-3-540-22286-6, Germany

van der Knaap, M. et al.. (2006). Vanishing white matter disease. *Lancet Neurol*, Vol.5, No.5, (May 2006), pp. 413-423, ISSN 1474-4422

van der Knaap, M. & Scheper, G. (July 2008). Megalencephalic leukoencephalopathy with subcortical cysts, In: GeneReviews, 24.02.2011, Available from http://www.ncbi.nlm.nih.gov/books/NBK1535/#mlc.Summary

Vargas, M. et al.. (December 2009). Magnetic resonance imaging of metabolic disease of the cerebral white matter. *Top Magn Reson Imaging*, Vol.20, No.6, (December 2009), pp. 333-341, ISSN 0899-3459

Varho, T. et al.. (1999). A new metabolite contributing to N-acetyl signal in 1H MRS of the brain in Salla disease. *Neurology*, Vol.52, No.8, (May 1999), pp. 1668-72, ISSN 0028-3878

Yager, J. et al.. (1988). CT-scan findings in an infant with glutaric aciduria type I. *Dev Med Child Neurol*, Vol.30, No.6, (December 1988), pp. 808-811, ISSN 0012-1622

Wenger, D. (August 2008). Krabbe disease, In: GeneReviews, 26.02.2011, Available from http://www.ncbi.nlm.nih.gov/books/NBK1238/#krabbe.Summary

Williams, R. et al.. (2006). Diagnosis of the neuronal ceroid lipofuscinoses: an update. *Biochim Biophys Acta,* Vol.1762, No.10, (October 2006), pp. 865-872, ISSN 0006-3002

Zarifi, M. et al.. (2001). Magnetic resonance spectroscopy and magnetic resonance imaging findings in Krabbe's disease. *J Child Neurol*, Vol.16, No.7, (July 2001), pp. 522-526, ISSN 0883-0738

Zhang, Y. et al.. (2006). Biochemical properties of human pantothenate kinase 2 isoforms and mutations linked to pantothenato kinase-associated neurodegeneration. *J Biol Chem*, Vol.281, No.1, (January 2006), pp. 107-114, ISSN

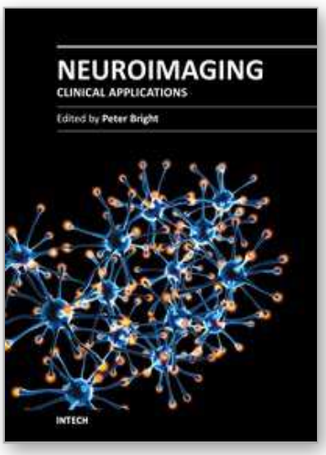

Neuroimaging - Clinical Applications
Edited by Prof. Peter Bright

ISBN 978-953-51-0200-7
Hard cover, 576 pages
Publisher InTech
Published online 09, March, 2012
Published in print edition March, 2012

Modern neuroimaging tools allow unprecedented opportunities for understanding brain neuroanatomy and function in health and disease. Each available technique carries with it a particular balance of strengths and limitations, such that converging evidence based on multiple methods provides the most powerful approach for advancing our knowledge in the fields of clinical and cognitive neuroscience. The scope of this book is not to provide a comprehensive overview of methods and their clinical applications but to provide a "snapshot" of current approaches using well established and newly emerging techniques.

How to reference
In order to correctly reference this scholarly work, feel free to copy and paste the following:

Carlos Casimiro, Paula Garcia, Miguel Cordeiro, Isabel Fineza, Teresa Garcia and Luísa Diogo (2012). Neuroimaging in Inborn Errors of Metabolism, Neuroimaging - Clinical Applications, Prof. Peter Bright (Ed.), ISBN: 978-953-51-0200-7, InTech, Available from: http://www.intechopen.com/books/neuroimaging-clinical-applications/neuroimaging-in-inborn-errors-of-metabolism

INTECH
open science | open minds

InTech Europe
University Campus STeP Ri
Slavka Krautzeka 83/A
51000 Rijeka, Croatia
Phone: +385 (51) 770 447
Fax: +385 (51) 686 166
www.intechopen.com

InTech China
Unit 405, Office Block, Hotel Equatorial Shanghai
No.65, Yan An Road (West), Shanghai, 200040, China
中国上海市延安西路65号上海国际贵都大饭店办公楼405单元
Phone: +86-21-62489820
Fax: +86-21-62489821

IntechOpen